Clim. Past Discuss., https://doi.org/10.5194/cp-2019-16
Manuscript under review for journal Clim. Past
Discussion started: 12 February 2019

Climate of the Past Discussions
Open Access
EGU

Climate changes in interior semi-arid Spain from the last interglacial to the late Holocene

Dongyang Wei[1,2], Penélope González-Sampériz[3], Graciela Gil-Romera[3], Sandy P. Harrison[1], I. Colin Prentice[4]

1: Department of Geography and Environmental Science, University of Reading, Whiteknights, Reading, RG6 6AB, UK
2: Masters Programme in Ecosystem and Environmental Change, Department of Life Sciences, Imperial College London, Ascot, SL5 7PY, UK
3: Instituto Pirenaico de Ecología-CSIC, Avda. Montañana 1005, 50059 Zaragoza, Spain
4: AXA Chair Programme in Biosphere and Climate Impacts, Department of Life Sciences, Imperial College London, Ascot, SL5 7PY, UK

Clim. Past Discuss., https://doi.org/10.5194/cp-2019-16
Manuscript under review for journal Clim. Past
Discussion started: 12 February 2019

Climate of the Past Discussions
Open Access
EGU

Abstract

The El Cañizar de Villarquemado sequence provides a palaeoenvironmental record from the western Mediterranean Basin spanning the interval from the last part of MIS6 to the late Holocene. The pollen and sedimentological records provide qualitative information about changes in temperature seasonality and moisture conditions. We use Weighted Averaging Partial Least-Squares (WA-PLS) regression to derive quantitative reconstructions of winter and summer temperature regimes from the pollen data, expressed in terms of the mean temperature of the coldest month (MTCO) and growing degree days above a baseline of 0° C (GDD_0) respectively. We also reconstruct a moisture index (MI), the ratio of annual precipitation to annual potential evapotranspiration, taking account of the effect of low CO_2 on water use efficiency. We find a rapid summer warming at the transition to MIS5. Summers were cold during MIS4 and MIS2, but some intervals in MIS3 were characterized by summers as warm as the warmest phases of MIS5 or the Holocene. However, MIS3 was not significantly warmer in winter than other intervals, and there was a gradual decline in winter temperature from MIS4 through MIS3 to MIS2. The pronounced changes in temperature seasonality during MIS5 and MIS1 are consistent with changes in summer insolation. The ecophysiological effects of changing CO_2 concentration through the glacial cycle has a significant impact on reconstructed MI. Conditions became progressively more humid during MIS5 and MIS4 was also relatively humid, while MIS3 was more arid. High MI values are reconstructed during the deglaciation and there was a pronounced increase in aridity during the Holocene. Changes in MI are anti-correlated with changes in GDD_0, with increased MI during intervals of summer warming indicating a strong influence of temperature on evapotranspiration. Although our main focus here is on longterm changes in climate, the Villarquemado record also shows millennial-scale changes corresponding to Dansgaard-Oeschger cycles.

Clim. Past Discuss., https://doi.org/10.5194/cp-2019-16
Manuscript under review for journal Clim. Past
Discussion started: 12 February 2019

Climate of the Past Discussions

1 Introduction

The modern climate of the western Mediterranean region is influenced by high pressure systems in summer and westerly storm tracks in winter, giving rise to a highly seasonal climate with dry summers, wetter winters and strong seasonal temperature contrasts. The region is sensitive to both extratropical and low-latitude influences, and therefore registers climate changes on glacial-interglacial time scales due to changes in ice sheet volume and on orbital time scales due to changes in insolation (Magri and Tzedakis, 2000; Rohling et al., 2013). Records from the western Mediterranean region also show abrupt climate changes during the glacial associated with the Dansgaard-Oeschger (D-O) cycles and Heinrich events (Sánchez-Goñi et al., 2002; Fletcher et al., 2010; Vegas et al., 2010; Moreno et al., 2012). In addition, continental records from the Iberian peninsula show abrupt changes during the late glacial and early Holocene (e.g. González-Sampériz et al., 2006; Moreno et al., 2012; Pérez-Sanz et al., 2013; Ramos-Román et al., 2018).

The El Cañizar de Villarquemado palaeolake (hereafter Villarquemado) is located in the semi-arid interior of the Iberian Peninsula (40.49°N, 1.29°W, 985 m a.s.l.), and provides a long, continuous pollen record that stretches from the end of the penultimate glaciation (Marine Isotope Stage 6, MIS6) through the last interglacial (MIS5), the last glaciation (MIS4, 3 and 2) and into MIS1 and the Holocene (Moreno et al., 2012; González-Sampériz et al., 2013; Aranbarri et al., 2014). The record has 30 radiocarbon, IRSL and OSL dates and a robust independent chronology constructed using Bayesian modelling (Valero-Garcés et al.). The length of the record and the quality of the age model make Villarquemado a uniquely important site to understand climate changes in Spain on both glacial-interglacial and orbital timescales. The only other record from Spain that spans this length of time is Padul (Pons and Reille, 1988; Camuera et al., 2018), in southern Spain. The chronology for the interval before 50 ka at Padul is based on amino-acid racemization and an assumption of constant sedimentation rates and is thus poorly constrained compared to the Villarquemado record. Most other long records from the Mediterranean region, including the classic site of Tenaghi Phillippon (Tzedakis et al., 2006; Milner et al., 2013) and the newer record from Lake Ohrid (Wagner et al., 2017; Sinopoli et al., 2018; Sinopoli et al., 2019), use some form of orbital tuning in constructing an age model. The only exception is Lago di Monticchio in central Italy (Allen et al., 2000; Allen and Huntley, 2009; Martin-Puertas et al., 2014; Allen and Huntley, 2018) – but while this has a highly resolved and independent chronology, the site is in a much wetter climate today than Villarquemado. Interglacial intervals in Lago di Monticchio are dominated by temperate deciduous trees whereas Villarquemado is characterized by evergreen trees and shrubs (González-Sampériz et al., 2013).

In this paper, we present a quantitative reconstruction of three bioclimatic variables: winter temperature (mean temperature of the coldest month, MTCO), growing-season warmth (growing degree days above a base level of 0°C, GDD_0) and a moisture index (the ratio of annual precipitation to annual potential evapotranspiration, MI) using the pollen record from Villarquemado and Weighted Averaging Partial Least-Squares regression (WA-PLS: ter Braak and Juggins, 1993). We apply a novel method of correcting MI to take account of the direct physiological influence of $[CO_2]$ on water use efficiency. Although Villarquemado is well dated, there are several intervals with poor pollen preservation, so we focus on the long-term evolution of climate rather than the evidence for abrupt climate changes. Finally, we compare our reconstructions with available pollen-based reconstructions from the wider Mediterranean region, and

Clim. Past Discuss., https://doi.org/10.5194/cp-2019-16
Manuscript under review for journal Clim. Past
Discussion started: 12 February 2019

discuss the implications of the reconstructed changes.

2 Methods

2.1 Modern pollen data

The modern pollen dataset (Fig. 1) consists of records from 6458 terrestrial sites. The bulk of the sites were derived from the European Modern Pollen Database (EMPD) v 3.0 (Davis et al., 2013) and the EMBSeCBIO (Eastern Mediterranean-Black Sea-Caspian corridor BIOmes) Initiative (Marinova et al., 2017). We included additional sites from various publications (Saadi and Bernard, 1991; de Klerk et al., 2009; Gruger and Jerz, 2010; Muller et al, 2010; Werner et al., 2010; Tarasov et al, 2011; Matthias et al., 2015; Niemeyer et al., 2015; Bell & Fletcher, 2016; Novenko et al., 2017) available from the European Pollen Database (http://www.europeanpollendatabase.net/) or Pangaea (https://www.pangaea.de/). We also included long-term pollen trap data. In addition, we included 73 modern surface samples from northern Spain (see Supplementary Information Table 1, and González-Sampériz, 1999; Garcia-Prieto, 2015; Aranbarri et al., 2015; Leunda et al., 2017; Rieradevall et al., 2018).

We standardised the taxonomy for the pollen data using Plants of the World Online (www.plantsoftheworldonline.org/) and the Integrated Taxonomic Information System (https://www.itis.gov/). We removed obligate aquatics (e.g. *Azolla*, *Lemna*, *Myriophyllum*), insectivorous plants (e.g. *Drosera*), parasitic plants (e.g. *Bartsia*) and introduced species (e.g. *Eucalyptus*, *Liquidambar*) assuming that the distribution of these plants is only partially related to climate. We also removed cultivated plants (e.g. *Avena*, *Cannabis*, *Hordeum*), although we retained taxa (e.g. *Olea, Prunus*) that can be cultivated but also occur in the wild. Even after these deletions, there are still many (1558) taxa in the modern data set. However, it cannot be assumed that all taxa have been identified consistently to the same level of taxonomic discrimination. A further problem is that discrimination of sub-types is unnecessary in regions where only one sub-type is present (e.g. it is not usually stated whether *Quercus* is deciduous or evergreen in northern Europe, where all the *Quercus* species present are deciduous). Some families are only represented by a single genus in the data set (e.g. *Verbena* is the only representative of the Verbenaceae, most other genera in this family are tropical); in such cases, preserving both family and genus is meaningless. Finally, although some herbaceous species are recognizable at species level, they do not occur in distinctive climate regimes, and thus preservation of these as individual species does not convey additional information about climate. We therefore reduced the original taxon list by amalgamating taxa into a manageable list. The amalgamation process was guided by palynological and ecological understanding of the pollen types and tested by constructing climate space diagrams for each original and amalgamated taxon using generalised additive models (GAMs).

The GAMs were implemented with the *mgcv* R package (Wood, 2017). The R implementation makes the selection of the smoothing parameters automatic (Guisan et al., 2002). We used a square root transformation of MI, as differences between MI values at the wet end are less important than differences at the dry end in terms of their effect on vegetation (Prentice et al., 2017). Logistic models were used in the first step of the GAMs. The fitted response surfaces show the concentration of the pollen taxon abundance in climate space. Interaction terms were not included, because we assume that each bioclimate variable independently influences the distribution of plant taxa and

Clim. Past Discuss., https://doi.org/10.5194/cp-2019-16
Manuscript under review for journal Clim. Past
Discussion started: 12 February 2019

vegetation types, following the logic of Wang et al. (2013). For visualization purposes, the 3D response surfaces of taxon abundance resulting from the GAM were portrayed as slices for low, medium and high values of GDD_0. Convex hulls, implemented with the *alphahull* and *ggplot2* packages in R (Pateiro-Lopez & Rodriguez-Casal, 2016, Wickham, 2016), were used to show the area where samples actually lie and thus avoid representing parts of the fitted surface that were not closely constrained by data.

Supplementary Table 2 provides the translation of the original taxa into the taxon list used in our analyses. The final taxon list (249 taxa) includes several layers of specificity: individual species, genera, sub-families, and families. All pollen data were transformed from raw counts to relative abundance prior to analysis. Amalgamated taxa that occur in less than 10 sites were not considered in the final analysis, which therefore only uses 196 taxa.

2.2 Modern climate data and derivation of bioclimatic variables

Climatological data (mean monthly temperature, precipitation, and fractional sunshine hours) were derived from the CRU CL v2.0 gridded dataset of modern (1961-1990) surface climate at 10 arc minute resolution (~18 km) (New et al., 2002). Geographically weighted regression (GWR) was carried out in ArcGIS (v10.3, ESRI, 2014) to correct for elevation differences between each pollen site and the corresponding grid cell. A fixed bandwidth kernel of 1.06° (~140km) was used because this optimized model diagnostics and reduced spatial clustering of residuals relative to other bandwidths. The climate of each pollen site was then estimated based on its longitude, latitude, and elevation. The mean temperature of the coldest month (MTCO) was taken directly from the GWR regression. Growing degree days above 0°C (GDD_0) were estimated from daily data using a mean-conserving interpolation (Rymes and Myers, 2001) of the monthly mean temperatures. The annual Moisture Index, defined as the ratio of annual precipitation to annual potential evapotranspiration (MI), was calculated for each pollen site using code modified from SPLASH v1.0 (Davis et al., 2017) based on daily values of precipitation, temperature and sunshine hours again obtained using a mean-conserving interpolation of the monthly values of each.

2.3 Statistical analyses

Canonical correspondence analysis (CCA; ter Braak, 1986; Legendre & Legendre, 2012) was used to perform a constrained ordination of the modern pollen data in response to the bioclimatic variables. CCA was implemented with the *vegan* package (Oksanen et al., 2017) in R (v3.3.1). We excluded predictors with variance inflation factors (VIFs), which give a measure of the multi-collinearity in predictors, higher than 20. The significance of the CCA model was computed with an ANOVA-like permutation test. The CCA allows an assessment of the degree to which the bioclimate variables reflect the main pattern of variability in the modern pollen data (Table 1).

2.4 Fossil pollen data

The Villarquemado palaeolake (González-Sampériz et al., 2013) is located in the Jiloca basin in the semi-arid region of north-eastern Spain (Fig. 1). The site is occupied today by a wetland and cultivated land. The surrounding vegetation is dominated by evergreen trees (*Quercus ilex*, *Q. coccifera, Q. faginea*) and xerophytic shrubs (e.g. *Rhamnus lycioides*, *Genista scorpius*, *Ephedra fragilis*, *Thymus vulgaris, T. zygis*). *Juniperus* (*J.*

Clim. Past Discuss., https://doi.org/10.5194/cp-2019-16
Manuscript under review for journal Clim. Past
Discussion started: 12 February 2019

Climate of the Past Discussions

thurifera, *J. communis*, *J. sabina*, *J. oxycedrus*) and *Pinus* (*P. sylvestris*, *P. pinaster*) occur at higher elevations. A 74m-long core, taken from the deepest part of the wetland, provides a pollen and sedimentological record back to MIS6 (Moreno et al., 2012; González-Sampériz et al, 2013; Aranbarri et al., 2014; Blas Valero-Garcés, submitted). The Bayesian age model is based on 30 ^{14}C, IRSL and OSL dates. The age model was constructed using BACON v2.2 (Blaauw and Christen, 2011). Full details of the age model are given in Valero-Garcés et al. Sedimentation rates are low during the initial part of the record and increase from the beginning of MIS2 onwards. There are intervals with poor pollen preservation between 16 085 and 22 328, 31 203 and 37 482, 43 112 and 50 103, and 87 895 and 93 809 cal yr BP. The average pollen sampling interval is ca 300 yr, increasing to ca 140 yr during MIS1. In general at least 300 pollen grains were counted per sample; no sample has less than 150 grains counted.

2. 5 WA-PLS

The modern bioclimatic and pollen data were used to develop pollen-climate transfer functions independently for MTCO, GDD_0 and MI using weighted-averaging partial least squares regression (WA-PLS) (ter Braak and Juggins, 1993). Like CCA, WA-PLS is based on the assumption that each taxon has a unimodal distribution in climate space. It is relatively robust to spatial autocorrelation, and uses model residuals to diminish bias and improve performance. WA-PLS was implemented with the *rioja* R package (Juggins, 2017). The performance of the calibration models was assessed through leave-one-out cross validation. The number of components used in each model was estimated through a randomisation *t*-test on the results (Van der Voet, 1994). We selected the component with the lowest root mean square error of prediction (RMSEP), but only if there was a significant improvement in RMSEP relative to a lower number of components – since including more components can result in over-fitting of the data so that model predictive value decreases (ter Braak et al., 1993). We checked that the final transfer functions had a high R^2 for prediction and a low maximum bias.

2.6 Correcting for changing [CO_2] concentration

In addition to affecting plants indirectly through changes in climate, atmospheric CO_2 concentration [CO_2] has a direct effect on plant physiological processes (Ehleringer et al., 1997; Farquhar, 1997; Prentice and Harrison, 2009). Increasing [CO_2] allows plants that use the standard C_3 pathway of photosynthesis (including temperate grasses and forbs, and nearly all trees) to assimilate more carbon while losing less water, implying an increase in water use efficiency (Bramley et al., 2013). Under conditions of low [CO_2], C_3 plants are less productive and this can also result in a shift in the balance of C_3 and C_4 plants. Pollen-based reconstructions that rely on calibration of pollen abundance against modern climate values do not account for the direct effects low [CO_2] on water use efficiency, and as a result reconstructions of moisture variables, such as precipitation and MI, register drier conditions than actually occurred (Prentice et al., 2017). Prentice et al. (2017) have developed a procedure to correct for this, and we have applied this correction using the implementation described in Cleator et al. (submitted). The procedure requires the specification of [CO_2] and mean annual temperature (MAT) at the site. We used the ice-core [CO_2] record (Bereiter et al., 2015), using a loess smoothing spline with a span of 0.1. We calculated MAT from the reconstructed MTCO and GDD_0 at a site (see Appendix 1). This calculation also allowed us to generate an estimate of the mean temperature of the warmest month (MTWA), which can then be used to generate a time series of temperature seasonality (MTWA−MTCO). We applied the correction to the downcore reconstructions of MI at Villarquemado.

Clim. Past Discuss., https://doi.org/10.5194/cp-2019-16
Manuscript under review for journal Clim. Past
Discussion started: 12 February 2019

Climate of the Past Discussions

3 Results

The CCA analysis shows a strong correlation between species abundance and the three climate variables in the modern pollen data set, with correlations of 0.83, 0.61 and 0.47 respectively (Table 1). The VIF scores for each bioclimatic variable are low (<6), indicating that they are reasonably independent, and the CCA shows that they each have an independent contribution to explaining the variation in abundance. This is confirmed by the ANOVA-like permutation test, which shows that the bioclimatic variables and the three variability axes are all significantly different from one another (Table 1).

For the construction of the WA-PLS regression, we used results from component 4 for MTCO and GDD_0 and component 3 for MI because these are the significant results with the lowest RMSE and highest R^2. The R^2 values are 0.69, 0.66 and 0.52 for MTCO, GDD_0 and MI respectively (Supplementary Table 3). Nevertheless, close examination of the downcore reconstructions showed there were anomalous peaks in reconstructed MI, particularly at the end of MIS5. These correspond to samples that have unusually high values of Poaceae and Polypodiales (Fig. 2), and where the sedimentary record indicates that these are likely to be aquatics. Both Poaceae and Polypodiales were therefore removed from the final WA-PLS model (Table 2). This made no change to the number of components or the goodness-of-fit of the model, but made the reconstructions of MI for the anomalous samples less extreme and more plausible (Fig. 3). It had no significant impact on the MTCO and GDD_0 reconstructions (Supplementary Fig. 1). We checked whether particularly high or low values in the temperature reconstructions were a result of anomalous characteristics of the pollen assemblages, specifically whether there was evidence of pollen degradation (as measured by the number of indeterminable grains in the sample) or the samples were characterized by low biodiversity (as measured by the N2 index: Hill, 1973). There was no evidence of a correlation between the abundance of indeterminable grains and anomalously high or low reconstruction values. However, depauperate samples tended to produce more extreme temperature values than adjacent more diverse sample (Supplementary Fig. 2). We therefore exclude samples with an N2 value <2 from the final reconstructions. Excluding samples with a value of <3 had little effect on the reconstructions but increased the patchiness of the reconstructions by removing a large number of samples.

The reconstructions (Fig. 4, Supplementary Table 4) show an increase in both summer (GDD_0) and winter (MTCO) temperature between 130 and 127 ka. There is a general trend for both summer and winter temperature to decline through MIS5, and although there are fluctuations, they do not correspond exactly with the chronological boundaries of sub-stages within MIS5 (Fig. 4; definition of stage and sub-stage boundaries in the Supplementary Table 5). Furthermore, the changes in summer and winter temperature are not in phase. Minimum winter temperatures occurred earlier than minimum summer temperature in MIS5e, so that winter temperatures were already increasing while summer temperatures continued to decrease after ca 120 ka. In contrast, during MIS5a, warming in summer occurred at broadly the same time as winter cooling such that the temperature seasonality was significantly enhanced between ca 80 and 70 ka. There was no pronounced cooling, either in summer or winter, at the transition into the glacial (Fig. 4). The record from both MIS3 and MIS 2 is not continuous and the available samples may show the response to millennial-scale events; thus it is difficult to characterise the general trends in temperature. However, MIS 3 appears to have been

Clim. Past Discuss., https://doi.org/10.5194/cp-2019-16
Manuscript under review for journal Clim. Past
Discussion started: 12 February 2019

Climate of the Past Discussions

somewhat warmer than both MIS2 and MIS4 in summer. MIS3 was not significantly warmer in winter than other intervals during the glacial, and indeed there was a gradual decline in winter temperature from MIS4 through MIS3 to MIS2. MIS 1 was characterized by a general warming trend in both summer and winter, although the reconstructions show considerable variability superimposed on this trend.

The implied increase in temperature seasonality during MIS5e, 5c, 5a and during the early part of MIS1 corresponds to increased seasonality in insolation compared to the present day (Fig. 5), primarily driven by high summer insolation. Insolation changes across the glacial were comparatively muted. Intervals of increased temperature seasonality during MIS3, therefore, cannot be explained by changes in the seasonality of insolation.

Conditions became progressively more humid from MIS5e through to MIS5c, while conditions were generally humid but variable during MIS5a (Fig. 4, Table 3). MIS4 was also relatively humid, while MIS3 was the most arid phase reconstructed during the glacial. However, the difference in reconstructed MI between MIS4 or MIS2 and MIS3 is not large. This reflects the fact that [CO_2] decreased throughout the glacial, so that the impact of the CO_2 correction becomes larger from MIS4 through MIS3 and into MIS2 (Supplementary Fig. 3). The influence of changing [CO_2] is most marked in comparatively dry climates (Fig. 6), which is why this effect has such an important influence on the reconstructions of MI at Villarquemado. The highest values of MI are reconstructed during the deglaciation and there was a pronounced increase in aridity during the Holocene. The reconstructed changes in MI are broadly anti-correlated with changes in GDD_0 ($r = -0.69$), with decreased MI during intervals of summer warming. This suggests that the changes in MI were largely driven by changes in evapotranspiration rather than changes in precipitation.

There are several abrupt changes shown in the reconstructions, most particularly during MIS5a and in the glacial period. Some of these (Supplementary Fig. 4) clearly correspond to D-O events, including D-O 20 (72.28-70.28 cal ka) and 19 (76.4-74 cal ka) in MIS5a and 9 (40.11-39.81 cal ka) and 8 (38.17-36.57 cal ka) in MIS3. Heinrich Stadial 2 (26.45-24.25 cal ka) also clearly corresponds to an interval of year-round cooling in our reconstructions. Gaps in the pollen record, and poor dating resolution in some parts of the record, preclude identification of all of the D-O and Heinrich events. However, where D-O events are registered, they were characterized by a marked increase in seasonality – this explains the apparently anomalous high seasonality recorded during some parts of the glacial (Fig. 5).

4 Discussion and Conclusion

The Villarquemado record is characterized by rapid warming in winter temperature of ca 5°C and an increase in the summer growing season of ca 2000 degree days over a period of ca 2-3 kyr during the transitions from MIS6 to MIS5e. Although there are fluctuations, there is an overall decline in both summer and winter temperature through MIS5. However, there is a major interval with poor pollen preservation during MIS5b, and this limits our ability to gain a complete picture of the evolution of climate during this interval. Temperatures reconstructions for MIS4, 3 and 2 do not appear to be

Clim. Past Discuss., https://doi.org/10.5194/cp-2019-16
Manuscript under review for journal Clim. Past
Discussion started: 12 February 2019

Climate of the Past Discussions

significantly lower than the end of MIS5, but this may be because the coldest intervals occur during the intervals of low pollen preservation in MIS 3 and 2. The Younger Dryas interval is marked by relatively cold summers. There was a gradual warming in both summer and winter through the Holocene. The broad-scale changes in moisture are in general coherent with changes in GDD_0, with warmer summer intervals characterised by drier conditions and colder summers by wetter conditions. However, the MI reconstructions indicate that the whole of the past ca 130 kyr was wetter than today. Rapid millennial-scale changes in temperature and moisture are superimposed on these longer-term trends, though not all D-O events can be identified in the Villarquemado record.

Many of the features of the Villaquemado record are shown in other quantitative reconstructions from the Mediterranean. Both the Monticchio (Allen et al., 2002; Allen and Huntley, 2009) and the Lake Ohrid (Sinopoli et al., 2019) record show rapid warming at the transition from MIS6 to MIS5e. This warming occurs over longer period in the Monticchio (ca 5kyr) and Ohrid (ca 7 kyr) records. Differences between the sub-stages of MIS5 are more pronounced in the Monticchio and Ohrid records than at Villarquemado. The comparison of modern analogue and WA-PLS reconstructions at Lake Ohrid shows that modern analogue reconstructions (and by implication the response-surface approach used at Monticchio) tend to produce stronger fluctuations, and this might contribute to explaining the more muted variability at Villarquemado. However, the pronounced cold, dry interval registered in Monticchio and Ohrid during 5b corresponds to an interval of low pollen preservation in Villarquemado. This, and the fact that the Villarquemado site lies at the warmer and drier end of the climate gradient across the Mediterranean, could contribute to the apparent differences between the sites.

The coldest interval at Monticchio during MIS 2 is also represented by a hiatus in Villarquemado. The Younger Dryas was characterised by cooler summers and wetter conditions at Villarquemado, but only a small decrease in winter temperature. The wetter conditions and the muted winter temperature response are consistent with the record from Monticchio (Allen and Huntley, 2009). However, the Holocene record from Monticchio is very different from the pattern of climate change shown at Villarquemado. Whereas the Villarquemado record is characterised by warming and drying, the Monticchio record shows summer cooling and relatively stable moisture levels after 10 ka. Thus, while there are some similarities between the available quantitative records from the Mediterranean, they each show distinctive features reflecting the complexity of climate changes across the region and differences in modern climate and vegetation. This complexity will only be resolved when more quantitative reconstructions, preferably using a consistent methodology, are available from the circum-Mediterranean region.

The temperature record at Villarquemado shows intervals of enhanced seasonality during MIS5 and MIS1, largely but not entirely driven by changes in GDD_0 (a reflection of summer temperature and the length of the growing season). We have shown that there is a good correlation between these intervals of enhanced seasonality and orbitally-forced changes in summer insolation. Insolation changes across the glacial were comparatively small and this is reflected in muted changes in temperature seasonality. Orbital forcing was not the only cause of enhanced seasonality at Villarquemado, since we also see enhanced seasonality during D-O events (e.g. D-O 9). However, enhanced seasonality during the D-O events appears to have been driven primarily by changes in winter temperature. On both orbital and millennial time scales,

Clim. Past Discuss., https://doi.org/10.5194/cp-2019-16
Manuscript under review for journal Clim. Past
Discussion started: 12 February 2019

changes in MI are generally anti-correlated with changes in GDD_0 presumably because increased summer temperature and/or increased length of the growing season led to increased evapotranspiration and hence reduced MI.

There are major gaps in the palynological record from Villarquemado because of intervals of poor pollen preservation during MIS5b, MIS3 and MIS2 (Fig. 2). The sedimentological record suggests that these were arid intervals, characterized by alluvial fan rather than lacustrine deposition, and oxidation of the sediments. A speleothem record from El Pindal (Moreno et al., 2010) also show hiatuses in formation during MIS2, consistent with our interpretation that the depositional hiatus at Villarquemado is indicative of pronounced aridity. Similar situations have been identified in other palynological sequences during arid intervals (Valero-Garcés et al., 2000, 2004; Vegas-Villarubía et al., 2013; González-Sampériz et al., 2004, 2005). Hyper-arid periods are a problem for pollen preservation and, while further work may improve the pollen record at Villarquemado, it is unlikely that we will be able to obtain a quantitative record of climate during such intervals. Nevertheless, Villarquemado provides the most complete and well-dated record from continental Iberia (González-Sampériz et al., 2010; Moreno et al., 2012) and it is important to document changes in the drier part of the circum-Mediterranean region.

All reconstruction methods that use modern pollen-climate relationships are sensitive to the choice of training data sets, vegetation diversity and the potential absence of analogue assemblages (Gavin et al., 2003; Jackson and Williams, 2004; Bartlein et al., 2011). However, the training data set that we have used contains more than 6000 samples and includes samples from very cold and very warm environments to allow reconstruction of climate both much warmer and much colder than today. Analysis of the GAMs for individual taxa also shows that they have ecologically plausible relationships with climate variables. We have shown that pollen preservation issues, as indicated by intervals when the number of indeterminable grains was higher than average, do not affect our reconstructions. However, our analyses show that intervals of very low biodiversity are often characterized by more extreme values than other intervals. We have taken this into account by screening the down-core samples and excluding samples that have very low diversity.

Much of the discussion about the lack of modern analogues has focused on interpretation of assemblages of species that are not found together today (Overpeck et al., 1985; Jackson and Williams, 2004; Williams and Shuman, 2008). However, one important non-analogue situation that is ignored in all previous reconstructions is the impact of $[CO_2]$ different from today on plant assemblages. This does not affect temperature reconstructions but has a significant effect on moisture-related variables such as precipitation or any moisture index (Prentice et al., 2017; Cleator et al., submitted). Taking the impact of $[CO_2]$ into account in our reconstructions reduces the variability of MI during glacial intervals. Prentice et al. (2017) showed that this correction produced a reconciliation of apparently contradictory interpretations of pollen and geomorphic data for hydroclimatic changes in southeastern Australia at the Last Glacial Maximum. Comparison of our reconstructions from Villarquemado with other hydroclimatic data would be useful to test the realism of the reconstructed MI changes.

The Villarquemado reconstructions provide a detailed picture of the response of western Mediterranean climate and vegetation to changes in external forcing in this sensitive region for a long time. It would be useful to generate quantitative

Clim. Past Discuss., https://doi.org/10.5194/cp-2019-16
Manuscript under review for journal Clim. Past
Discussion started: 12 February 2019

Climate of the Past Discussions
Open Access
EGU

reconstructions from other long records, since preliminary comparisons with Lago di Monticchio and Lake Ohrid indicate some complexity in the response of climate to changes in external forcing within the circum-Mediterranean region. However, given that the largest impact of glacial-interglacial changes in atmospheric circulation is likely to be on precipitation and plant-available moisture, it will be important to take account of the impact of changing [CO_2] in these reconstructions.

Acknowledgements

DW and SPH acknowledge support from the ERC-funded project GC2.0 (Global Change 2.0: Unlocking the past for a clearer future, grant no. 694481). PG-S, GG-R and SPH acknowledge support from the Spanish Ministerio de Economia y Competitividad for the project CGL2015-69160R "Dinámica, Monitorización y Calibración de la vegetación Mediterránea en respuesta al Calentamiento Global en series temporales largas (DINAMO3), as well as for CGL2012-33063 and CGL2009-07992. ICP acknowledges support from the ERC-funded project Re-inventing Ecosystem and Land-surface Models (REALM), grant no. 787203. This research is a contribution to the AXA Chair Programme in Biosphere and Climate Impacts and the Imperial College initiative on Grand Challenges in Ecosystems and the Environment (ICP). We thank Jon Lloyd for advice on the implementation of convex hulls, and Maria Dance for the implementation of GWR. We also thank the PaleoIPE team for multi-proxy reconstruction and discussion regarding Villarquemado sequence; Maria Leunda, Josu Aranbarri and Héctor Romanos for providing additional surface pollen samples; and Miguel Sevilla Callejo for the Iberian Peninsula and Villarquemado vegetation maps of Figure 1.

Clim. Past Discuss., https://doi.org/10.5194/cp-2019-16
Manuscript under review for journal Clim. Past
Discussion started: 12 February 2019

References

Allen, J. R. M. and Huntley, B.: Last interglacial palaeovegetation, palaeoenvironments and chronology: A new record from Lago Grande di Monticchio, southern Italy, Quaternary Sci. Rev., 28, 1521–1538, https://doi.org/10.1016/j.quascirev.2009.02.013, 2009.

Allen, J. R. M. and Huntley, B.: Effects of tephra falls on vegetation: A Late-Quaternary record from southern Italy, J. Ecol., 106, 2456–2472, https://doi.org/10.1111/1365-2745.12998, 2018.

Allen, J. R. M., Watts, W. A., and Huntley, B.: Weichselian palynostratigraphy, palaeovegetation and palaeoenvironment; the record from Lago Grande di Monticchio, southern Italy, Quatern. Int., 73/74, 91-110, https://doi.org/10.1016/s1040-6182(00)00067-7, 2000.

Aranbarri, J., González-Sampériz, P., Valero-Garcés, B., Moreno, A., Gil-Romera, G., Sevilla-Callejo, M., García-Prieto, E., Di Rita, F., Mata, M. P., Morellón, M., Magri, D., Rodríguez-Lazaro, J., and Carrion, J. S.: Rapid climatic changes and resilient vegetation during the Lateglacial and Holocene in a continental region of south-western Europe, Global Planet. Change, 114, 50-65, https://doi.org/10.1016/j.gloplacha.2014.01.003, 2014.

Aranbarri, J., González-Sampériz, P., Iriarte, E., Moreno, A., Rojo-Guerra, M., Peña-Chocarro, L., Valero-Garcés, B., Leunda, M., García-Prieto, E., Sevilla-Callejo, M., Gil-Romera, G., Magri, D., and Rodríguez-Lázaro, J.: Human–landscape interactions in the Conquezuela–Ambrona Valley (Soria, continental Iberia): From the early Neolithic land use to the origin of the current oak woodland, Palaeogeogr. Palaeocl., 436, 41-57, https://doi.org/10.1016/j.palaeo.2015.06.030, 2015.

Bartlein, P. J., Harrison, S. P., Brewer, S., Connor, S., Davis, B. A. S., Gajewski, K., Guiot, J., Harrison-Prentice, T. I., Henderson, A., Peyron, O., Prentice, I. C., Scholze, M., Seppä, H., Shuman, B., Sugita, S., Thompson, R. S., Viau, A. E., Williams, J., and Wu, H.: Pollen-based continental climate reconstructions at 6 and 21 ka: a global synthesis, Clim. Dyn., 37, 775-802, https://doi.org/10.1007/s00382-010-0904-1, 2011.

Bell, B.A. and Fletcher, W. J.: Modern surface pollen assemblages from the Middle and High Atlas, Morocco: Insights into pollen representation and transport, Grana, 55, 286-301, https://doi.org/10.1080/00173134.2015.1108996, 2016.

Bereiter, B., Eggleston, S., Schmitt, J., Nehrbass-Ahles, C., Stocker, T. F., Fischer, H., Kipfstuhl, S., and Chappellaz, J.: Revision of the EPICA Dome C CO_2 record from 800 to 600 kyr before present, Geophys. Res. Lett., 42, 542–549, https://doi.org/10.1002/2014gl061957, 2015.

Blaauw, M. and Christen, J. A.: Flexible paleoclimate age-depth models using an autoregressive gamma process, Bayesian Anal., 6, 457-474, http://doi.org/10.1214/11-BA618, 2011.

Bramley, H., Turner, N., and Siddique, K.: Water use efficiency, in: Genomics and Breeding for Climate-Resilient Crops, Springer, Berlin, Heidelberg, Germany, 225-268, https://doi.org/10.1007/978-3-642-37048-9_6, 2013.

Camuera, J., Jiménez-Moreno, G., Ramos-Román, M. J., García-Alix, A., Toney, J. L., Anderson, R. S., Jiménez-Espejo, F., Kaufman, D., Bright, J., Webster, C., Yanes, Y., Carrión, J. S., Ohkouchi, N., Suga, H., Yamame, M., Yokoyama, Y., and Martínez-Ruiz, F.: Orbital-scale environmental and climatic changes recorded in a new ~200,000-year-long multiproxy sedimentary record from Padul, southern Iberian Peninsula, Quaternary Sci. Rev., 198, 91-114,

https://doi.org/10.1016/j.quascirev.2018.08.014, 2018.

Cleator, S. F., Harrison, S. P., Nichols, N. K., Prentice, I. C., and Roustone, I.: A method for generating coherent spatially explicit maps of seasonal palaeoclimates from site-based reconstructions, J. Adv. Model. Earth Sy., submitted.

Davis, B. A. S., Zanon, M., Collins, P., Mauri, A., Bakker, J., Barboni, D., Barthelmes, A., Beaudouin, C., Bjune, A. E., Bozilova, E., Bradshaw, R. H. W., Brayshay, B. A., Brewer, S., Brugiapaglia, E., Bunting, J., Connor, S. E., de Beaulieu, J., Edwards, K., Ejarque, A., Fall, P., Florenzano, A., Fyfe, R., Galop, D., Giardini, M., Giesecke, T., Grant, M. J., Guiot, J., Jahns, S., Jankovska, V., Juggins, S., Kahrmann, M., Karpin´ska-Kołaczek, M., Kołaczek, P., Kuhl, N., Kunes, P., Lapteva, E. G., Leroy, S. A. G., Leydet, M., Saez, J. A. L., Masi, A., Matthias, I., Mazier, F., Meltsov, V., Mercuri, A. M., Miras, Y., Mitchell, F. J. G., Morris, J. L., Naughton, F., Nielsen, A. B., Novenko, E., Odgaard, B., Ortu, E., Overballe-Petersen, M. V., Pardoe, H. S., Peglar, S. M., Pidek, I. A., Sadori, L., Seppa, H., Severova, E., Shaw, H., ta-Musznicka, J. S., Theuerkauf M., Tonkov, S., Veski, S., van der Knaap, W. O., van Leeuwen, J. F. N., Woodbridge, J., Zimny, M., and Kaplan, J. O.: The European Modern Pollen Database (EMPD) project, Veg. Hist. Archaeobot., 22, 521–530, https://doi.org/10.1007/s00334-012-0388-5, 2013.

Davis, T. W., Prentice, I. C., Stocker, B. D., Thomas, R. T., Whitley, R. J., Wang, H., Evans, B. J., Gallego-Sala, A. V., Sykes, M. T., and Cramer, W.: Simple process-led algorithms for simulating habitats (SPLASH v.1.0): Robust indices of radiation, evapotranspiration and plant-available moisture, Geosci. Model Dev., 10, 689-708, https://doi.org/10.5194/gmd-10-689-2017, 2017.

de Klerk, P., Haberl, A., Kaffke, A., Krebs, M., Matchutadze, I., Minke, M., Schulz, J., and Joosten, H.: Vegetation history and environmental development since ca 6000 cal yr BP in and around Ispani 2 (Kolkheti lowlands, Georgia), Quaternary Sci. Rev., 28, 890-910, https://doi.org/10.1016/j.quascirev.2008.12.005, 2009.

Ehleringer, J. R., Cerling, T. E., and Helliker, B. R.: C_4 photosynthesis, atmospheric CO_2 and climate, Oecologia, 112, 285–299, https://doi.org/10.1007/s004420050311, 1997.

ESRI, ArcGIS Desktop: Release 10.3, Redlands, CA: Environmental System Research Institute, 2014.

Farquhar, G. D.: Climate change: Carbon dioxide and vegetation, Science, 278, 1411, https://doi.org/10.1126/science.278.5342.1411, 1997.

Fletcher, W., Sanchez-Goñi, M. F., Allen, J. R. M., Cheddadi, R., Combourieu Nebout, N., Huntley, B., Lawson, I., Londeix, L., Magri, D., Margari, V., Müller, U. C., Naughton, F., Novenko, E., Roucoux, K., and Tzedakis, P. C.: Millennial-scale variability during the last glacial in vegetation records from Europe, Quaternary Sci. Rev., 29, 2839-2864, https://doi.org/10.1016/j.quascirev.2009.11.015, 2010.

García-Prieto, E.: Dinámica de la Vegetación mediterránea en el NE Peninsular: la Secuencia de El Cañizar de Villarquemado (Teruel). Ph.D. thesis, University of Zaragoza, Spain, 359 pp., 2015.

Gavin, D. G., Oswald, W. W., Wahl, E. R., and Williams, J. W.: A statistical approach to evaluating distance metrics and analog assignments for pollen records, Quaternary Res., 60, 356–367, https://doi.org/10.1016/s0033-5894(03)00088-7, 2003.

González-Sampériz, P.: Análisis del polen subactual en la cueva de En Pardo (Planes, Alicante), in: Avances en el Estudio del Cuaternario español: (Secuencias, Indicadores paleambientales y Evolución de Procesos), edited by: Roqué, C. and Lluís Pallí Buxó, Universitat de Girona, Spain, 307-316, 1999.

González-Sampériz, P., Valero-Garcés, B. L., and Carrión, J. S.: Was the Ebro valley a glacial refugium for temperate trees?, Anales de Biología, 26, 13-20, 2004.

González-Sampériz, P., Valero-Garcés, B. L., Carrión, J. S., Peña-Monné, J. L., García-Ruiz, J. M., and Martí-Bono, C.: Glacial and Lateglacial vegetation in northeastern Spain: New data and a review, Quatern. Int., 140–141, 4–20, https://doi.org/10.1016/j.quaint.2005.05.006, 2005.

González-Sampériz, P., Valero-Garcés, B. L., Moreno, A., Jalut, G., García-Ruiz, J. M., Martí-Bono, C., Delgado-Huertas, A., Navas, A., Otto, T., and Dedoubat, J. J.: Climate variability in the Spanish Pyrenees during the last 30,000 yr revealed by the El Portalet sequence, Quaternary Res., 66, 38-52, https://doi.org/10.1016/j.yqres.2006.02.004, 2006.

González-Sampériz, P., García-Prieto, E., Aranbarri, J., Valero-Garcés, B. L., Moreno, A., Gil-Romera, G., Sevilla-Callejo, M., Santos, L., Morellón, M., Mata, M. P., Andrade, A., and Carrión, J. S.: Reconstrucción paleoambiental del último ciclo glacial-interglacial en la Iberia continental: La secuencia del cañizar de Villarquemado (Teruel). Cuadern. Inve. Investig., 39, 49-76, https://doi.org/10.18172/cig.1999, 2013.

González-Sampériz, P., Leroy, S. A. G., Carrión, J. S., Fernández, S., García-Antón, M., Gil-García, M. J., Uzquiano, P., Valero-Garcés, B., and Figueiral, I.: Steppes, savannahs, forests and phytodiversity reservoirs during the Pleistocene in the Iberian Peninsula, Rev. Palaeobot. Palyno., 162, 427-457, 2010.

Grüger, E. and Jerz, H.: Untersuchung einer Doline auf dem Zugspitzplatt: Ein palynologischer Beitrag zur holozänen Gletschergeschichte im Wettersteingebirge, E&G Quaternary Sci. J., 59, 66-75, https://doi.org/10.3285/eg.59.1-2.06, 2010.

Guisan, A., Edwards, T. C., and Hastie, T.: Generalized linear and generalized additive models in studies of species distributions: Setting the scene, Ecol. Model., 157, 89-100, https://doi.org/10.1016/s0304-3800(02)00204-1, 2002.

Hill, M. O.: Diversity and evenness: A unifying notation and its consequences, Ecology, 54, 427-432, https://doi.org/10.2307/1934352, 1973.

Jackson, S. T. and Williams, J. W.: Modern analogs in Quaternary palaeoecology: Here today, gone yesterday, gone tomorrow? Annu. Rev. Earth Pl. Sc., 32, 495–537, https://doi.org/10.1146/annurev.earth.32.101802.120435, 2004.

Juggins, S.: rioja: Analysis of quaternary science data, CRAN, available at: http://cran.r-project.org/package=rioja (last access: 19 January 2019), 2017.

Legendre, P. and Legendre, L.: Numerical Ecology, 3rd edn, Elsevier Science, Amsterdam, The Netherlands, 2012.

Leunda, M., González-Sampériz, P., Gil-Romera, G., Aranbarri, J., Moreno, A., Oliva-Urcia, B., Sevilla, M., and Valero-Garcés, B. L.: The Late-Glacial and Holocene Marboré Lake sequence (2612 m a.s.l., Central Pyrenees, Spain): Testing high altitude sites sensitivity to millennial scale vegetation and climate variability, Global Planet. Change, 157, 214-231, https://doi.org/10.1016/j.gloplacha.2017.08.008, 2017.

Magri, D. and Tzedakis, P. C.: Orbital signatures and long-term vegetation patterns in the Mediterranean, Quatern. Int., 73/74, 69–78, https://doi.org/10.1016/S1040-6182(00)00065-3, 2000.

Marinova, E., Harrison, S. P., Bragg, F., Connor, S., de Laet, V., Leroy, S., Mudie, P., Atanassova, J., Bozilova , E., Caner, H., Cordova, C., Djamali, M., Filipova-Marinova, M., Gerasimenko, N., Kouli, K., Kotthoff, U., Kvavadze, E., Lazarova, M., Novenko, E., Ramezani, E., Röpke, A., Shumilovskikh, L., Tantau, I., and Tonkov, S.: Pollen-derived biomes in the eastern Mediterranean-Black Sea-Caspian corridor, J. Biogeogr., 45, 484–499,

https://doi.org/10.1111/jbi.13128, 2017.

Martin-Puertas, C., Brauer, A., Wulf, S., Ott, F., Lauterbach, S., and Dulski, P.: Annual proxy data from Lago Grande di Monticchio (southern Italy) between 76 and 112 ka: new chronological constraints and insights on abrupt climatic oscillations, Clim. Past, 10, 2099-2114, https://doi.org/10.5194/cp-10-2099-2014, 2014.

Martín-Puertas, C., Valero-Garcés, B. L., Mata, M. P., González-Sampériz, P., Bao, R., Moreno, A., and Stefanova, V.: Arid and humid phases in southern Spain during the last 4000 years: the Zoñar Lake record, Córdoba, The Holocene, 18, 907-921, https://doi.org/10.1177/0959683608093533, 2008.

Matthias, I., Semmler, M. S. S., and Giesecke, T.: Pollen diversity captures landscape structure and diversity, J. Ecol., 103, 880-890, https://doi.org/10.1111/1365-2745.12404, 2015.

Milner, A. M., Müller, U. C., Roucoux, K. H., Collier, R. E. L., Pross, J., Kalaitzidis, S., Christanis, K., and Tzedakis, P. C.: Environmental variability during the Last Interglacial: a new high-resolution pollen record from Tenaghi Philippon, Greece, J. Quaternary Sci., 28, 113-117, https://doi.org/10.1002/jqs.2617, 2013.

Moreno, A., Valero-Garcés, B. L., González-Sampériz, P., and Rico, M.: Flood response to rainfall variability during the last 2000 years inferred from the Taravilla Lake record (Central Iberian Range, Spain), J. Paleolimnol., 40, 943-961, http://doi.org/10.1007/s10933-008-9209-3, 2008.

Moreno, A., Stoll, H. M., Jiménez Sánchez, M., Cacho, I., Valero-Garcés, B. L. , Ito, E., and Edwards, L. R.: A speleothem record of glacial (25-11.6 kyr BP) rapid climatic changes from northern Iberian Peninsula, J. Quaternary Sci., 71, 218-231, http://doi.org/10.1016/j.gloplacha.2009.10.002, 2010.

Moreno, A., González-Sampériz, P., Morellón, M., Valero-Garcés, B. L., and Fletcher, W. J.: Northern Iberian abrupt climate change dynamics during the last glacial cycle: A view from lacustrine sediments, Quat. Sci. Rev., 36, 139-153, https://doi.org/10.1016/j.quascirev.2010.06.031, 2012.

Müller, S., Tarasov, P., Andreev, A. A., Tutken, T., Gartz, S., and Diekmann, B.: Late Quaternary vegetation and environments in the Verkhoyansk Mountains region (NE Asia) reconstructed from a 50-kyr fossil pollen record from Lake Billyakh, Quat. Sci. Rev., 29, 2071-2086, https://doi.org/10.1016/j.quascirev.2010.04.024, 2010.

Niemeyer, B., Klemm, J., Pestryakova, L. A., and Herzschuh, U.: Relative pollen productivity estimates for common taxa of the northern Siberian Arctic, Rev. Palaeobot. Palyno., 221, 71-82, https://doi.org/10.1016/j.revpalbo.2015.06.008, 2015.

New M., Lister D., Hulme M., and Makin I.: A high-resolution data set of surface climate over global land areas, Clim. Res., 21, 1-25, http://doi.org/10.3354/cr021001, 2002.

Novenko, E., Mazei, N., and Kusilman, M.: Tree pollen representation in surface pollen assemblages from different vegetation zones of European Russia, Ecological Questions, 26, 61–65, http://doi.org/10.12775/EQ.2017.018, 2017.

Oksanen, J., Blanchet, F. G., Friendly, M., Kindt, R., Legendre, P., McGlinn, D., Minchin, P. R., O'Hara, R. B., Simpson, G. L., Solymos, P., Stevens, M. H. H., Szoecs, E., and Wagner, H.: vegan: Community Ecology Package, CRAN, available at: https://CRAN.R-project.org/package=vegan (last access: 19 January 2019), 2017.

Pateiro-Lopez, B. and Rodriguez-Casal, A.: alphahull: Generalization of the Convex Hull of a Sample of Points in the Plane, CRAN, available at: https://CRAN.R-project.org/package=alphahull (last access: 19 January 2019), 2016.

694 Pérez-Sanz, A.: Holocene climate, vegetation and human impact in the Western
695 Mediterranean inferred from Pyrenean lake records and climate models. Ph.D.
696 thesis, University of Zaragoza, Spain, 194 pp., 2014.
697 Pérez-Sanz, A., González-Sampériz, P., Moreno, A., Valero-Garcés, B., Gil-Romera,
698 G., Rieradevall, M., Tarrats, P., Lasheras-Álvarez, L., Morellón, M., Belmonte,
699 A., Sancho, C., Sevilla-Callejo, M., and Navas, A.: Holocene climate variability,
700 vegetation dynamics and fire regime in the central Pyrenees: the Basa de la
701 Mora sequence (NE Spain), Quat. Sci. Rev., 73, 149-169,
702 https://doi.org/10.1016/j.quascirev.2013.05.010, 2013.
703 Pons, A. and Reille, M.: The Holocene- and upper Pleistocene pollen record from Padul
704 (Granada, Spain): A new study, Palaeogeogr. Palaeocl., 66, 243-263,
705 https://doi.org/10.1016/0031-0182(88)90202-7, 1988.
706 Prentice, I. C. and Harrison, S. P.: Ecosystem effects of CO_2 concentration: Evidence
707 from past climates, Clim. Past, 5, 297-307, https://doi.org/10.5194/cp-5-297-
708 2009, 2009.
709 Prentice, I. C., Cleator, S. F., Huang, Y. F., Harrison, S. P., and Roulstone, I.:
710 Reconstructing ice–age palaeoclimates: Quantifying low-CO_2 effects on plants,
711 Global Planet. Change, 149, 166-176,
712 https://doi.org/10.1016/j.gloplacha.2016.12.012, 2017.
713 Ramos-Román, M. J., Jiménez-Moreno, G., Camuera, J., García-Alix, A., Anderson, R.
714 S., Jiménez-Espejo, F. J., Sachse, D., Toney, J. L., Carrión, J. S., Cole Webster,
715 C., and Yanes, Y.: Millennial-scale cyclical environment and climate variability
716 during the Holocene in the western Mediterranean region deduced from a new
717 multi-proxy analysis from the Padul record (Sierra Nevada, Spain), Global
718 Planet. Change, 168, 35-53, https://doi.org/10.1016/j.gloplacha.2018.06.003,
719 2018.
720 Rieradevall, M., González-Sampériz, P., Pérez-Martínez, C., Tarrats, P., Leunda, M.,
721 Aranbarri, J., Gil-Romera, G., and Prat, N.: Evaluación y seguimiento del
722 cambio global en dos lagos de alta montaña (Enol y Marboré) de la red española
723 de Parques Nacionales: indicadores biológicos (CLAM2), in: Monográfico
724 Proyectos de investigación en Parques Nacionales: 2012-2015, 307-325, 2018.
725 Rohling, E., Grant, K., Roberts, A., and Larrasoaña, J.: Paleoclimate variability in the
726 Mediterranean and Red Sea regions during the Last 500,000 Years: Implications
727 for hominin migrations, Curr. Anthropol., 54, 183-201,
728 https://doi.org/10.1086/673882, 2013.
729 Rymes, M. D. and Myers, D. R.: Mean preserving algorithm for smoothly interpolating
730 averaged data, Sol. Energy, 71, 225-231, https://doi.org/10.1016/S0038-
731 092X(01)00052-4, 2001.
732 Saadi, F. and Bernard, J.: Rapport entre la pluie pollinique actuelle, le climat et la
733 vegetation dans les steppes à Artemisia et les milieu limitrophes au Maroc,
734 Palaeoecol. Africa, 22, 67-86, 1991.
735 Sánchez-Goñi, M. F., Cacho, I., Turon, J. L., Guiot, J., Sierro, F. J., Peypouquet, J. P.,
736 Grimalt, J. O., and Shackleton, N.J.: Synchroneity between marine and
737 terrestrial responses to millennial scale climatic variability during the last
738 glacial period in the Mediterranean region, Clim. Dynam., 19, 95-105,
739 https://doi.org/10.1007/s00382-001-0212-x, 2002.
740 Sinopoli, G., Masi, A., Regattieri, E., Wagner, B., Francke, A., Peyron, O., and Sadori,
741 L.: Palynology of the Last Interglacial Complex at Lake Ohrid:
742 Palaeoenvironmental and palaeoclimatic inferences, Quat. Sci. Rev., 180, 177-
743 192, https://doi.org/10.1016/j.quascirev.2017.11.013, 2018.
744 Sinopoli, G., Peyron, O., Masi, A., Holtvoeth, J., Francke, A., Wagner, B., and Sadori,
745 L.: Pollen-based temperature and precipitation changes in the Ohrid Basin

(western Balkans) between 160 and 70 ka, Clim. Past, 15, 53-71, https://doi.org/10.5194/cp-15-53-2019, 2019.

Tarasov, P. E., Nakagawa, T., Demske, D., Österle, H., Igarashi, Y., Kitagawa, J., Mokhova, L., Bazarova, V., Okuda, M., Gotanda, K., Miyoshi, N., Fujiki, T., Takemura, K., Yonenobu, H., and Fleck, A.: Progress in the reconstruction of Quaternary climate dynamics in the Northwest Pacific: A new modern analogue reference dataset and its application to the 430-kyr pollen record from Lake Biwa, Earth-sci. Rev, 108, 64-79, https://doi.org/10.1016/j.earscirev.2011.06.002, 2011.

ter Braak, C. J. F.: Canonical Correspondence Analysis: A new eigenvector technique for multivariate direct gradient analysis, Ecology, 67, 1167-1179, https://doi.org/10.2307/1938672, 1986.

ter Braak, C. J. F. and Juggins, S.: Weighted averaging partial least squares regression (WA-PLS): An improved method for reconstructing environmental variables from species assemblages, Hydrobiologia, 269, 485-502, https://doi.org/10.1007/BF00028046, 1993.

Tzedakis, P. C., Hooghiemstra, J. F., and Palike, H.: The last 1.35 million years at Tenaghi Philippon: revised chronostratigraphy and long-term vegetation trends, Quat. Sci. Rev., 25, 3416-3430, https://doi.org/10.1016/j.quascirev.2006.09.002, 2006.

Valero-Garcés, B. L., González-Sampériz, P., Delgado-Huertas, A., Navas, A., Machín, J., and Kelts, K.: Lateglacial and Late Holocene environmental and vegetational change in Salada Mediana, central Ebro Basin, Spain, Quatern. Int., 73–74, 29–46, https://doi.org/10.1016/S1040-6182(00)00063-X, 2000.

Valero-Garcés, B. L, González-Sampériz, P., Navas, A., Machín, J., Delgado-Huertas, Peña-Monne, J. L., Sancho-Marcén, C., Stevenson, A., and Davis, B. A. S.: Paleohydrological fluctutations and steppe vegetation during the last glacial maximum in the Central Ebro valley (N.E. Spain). Quatern. Int., 122, 43-55, https://doi.org/10.1016/j.quaint.2004.01.030, 2004.

Valero-Garces, B. L., González-Sampériz, P., Gil-Romera, G. Benito, B., Moreno, A., Oliva-Urcia, B., Aranbarri, J., García-Prieto, E., Frugone-Álvarez, M., Morellon Marteles, M., Arnold, L., Demuro, M., Hardiman, M., Blockley, S., and Lane, C.: A multi-dating approach to age-modelling long continental records: the 135 ka El Cañizar de Villarquemado sequence (NE Spain), Quat. Geochronol., submitted.

Van der Voet, H.: Comparing the predictive accuracy of models using a simple randomization test, Chemometr. Intell. Lab., 25, 313-323, https://doi.org/10.1016/0169-7439(94)85050-X, 1994.

Vegas, J., Ruiz-Zapata, B., Ortiz, J. E., Galán, L., Torres, T., García-Cortés, Á., Gil García, M. J., Pérez-González, A., and Gallardo-Millán, J. L.: Identification of arid phases during the last 50 cal. ka BP from the Fuentillejo maar-lacustrine record (Campo de Calatrava Volcanic Field, Spain), J. Quaternary Sci., 25, 1051-1062, https://doi.org/10.1002/jqs.1262, 2010.

Vegas-Vilarrúbia, T., González-Sampériz, P., Morellón, M., Gil-Romera, G., Pérez-Sanz, A., and Valero-Garcés, B.: Diatom and vegetation responses to Late Glacial and Early Holocene climate changes at Lake Estanya (Southern Pyrenees, NE Spain), Palaeogeogr. Palaeocl., 392, 335–349, https://doi.org/10.1016/j.palaeo.2013.09.011, 2013.

Wagner, B., Wilke, T., Francke, A., Albrecht, C., Baumgarten, H., Bertini, A., Combourieu-Nebout, N., Cvetkoska, A. D., Addabbo, M., Donders, T. H., Foller, K., Giaccio, B., Grazhdani, A., Hauffe, T., Holtvoeth, J., Joannin, S., Jovanovska, E., Just, J., Kouli, K., Koutsodendris, A., Krastel, S., Lacey, J. H.,

Leicher, N., Leng, M. J.,Levkov, Z., Lindhorst, K., Masi, A., Mercuri, A. M., Nomade, S., Nowaczyk, N., Panagiotopoulos, K., Peyron, O., Reed, J. M., Regattieri, E., Sadori, L., Sagnotti, L., Stelbrink, B., Sulpizio, R., Tofilovska, S., Torri, P., Vogel, H., Wagner, T., Wagner-Cremer, F., Wolff, G. A., Wonik, T., Zanchetta, G., and Zhang, X. S.: The environmental and evolutionary history of Lake Ohrid (FYROM/Albania): Interim results from the SCOPSCO deep drilling project, Biogeosciences, 14, 2033-2054, https://doi.org/10.5194/bg-14-2033-2017, 2017.

Wang, H., Prentice, I. C., Keenan, T. F., Davis, T. W., Wright, I. J., Cornwell, W. K., Evans, B. J., and Peng, C.: Towards a universal model for carbon dioxide uptake by plants, Nat. Plants, 3, 734-741, https://doi.org/10.1038/s41477-017-0006-8, 2017.

Werner, K., Tarasov, P. E., Andreev, A. A., Müller, S., Kienast, F., Zech, M., Zech, W., and Diekmann, B.: A 12.5-kyr history of vegetation dynamics and mire development with evidence of Younger Dryas larch presence in the Verkhoyansk Mountains, East Siberia, Russia, Boreas, 39, 56-68, https://doi.org/10.1111/j.1502-3885.2009.00116.x, 2010.

Wickham, H.: ggplot2: Create Elegant Data Visualisations Using the Grammar of Graphics, CRAN, available at: https://CRAN.R-project.org/package=ggplot2 (last access: 19 January 2019)， 2016.

Wood, S.: mgcv: Mixed GAM Computation Vehicle with Automatic Smoothness Estimation, CRAN, available at: https://CRAN.R-project.org/package=mgcv (last access: 19 January 2019), 2017.

Clim. Past Discuss., https://doi.org/10.5194/cp-2019-16
Manuscript under review for journal Clim. Past
Discussion started: 12 February 2019

Figures and Table Captions

Figure 1. Location of modern pollen samples and fossil pollen site. (a) Map of the Iberian Peninsula showing the location of Villarquemado superimposed on a simplified elevation map of the region. (b) Vegetation map of Villarquemado area showing dominant tree species, surface area of the basin and location of the core site. (c) Map showing the location of Villarquemado and the distribution of modern pollen samples. The background map shows mean temperature of the coldest month (MTCO, °C).

Figure 2: Simplified stratigraphic and pollen diagram from Villarquemado. The first column shows changes in stratigraphy, including the alternation between lacustrine and non-lacustrine conditions. The simplified pollen diagram shows the changing abundance of Mediterranean and steppe taxa. We also show the changing abundance of Poaceae and Polypodiales. The final column shows the biodiversity index (Hill's N2).

Figure 3: The impact of removing Poaceae and Polypodiales from the taxon set on reconstructions of moisture index (the ratio of annual precipitation to annual potential evapotranspiration, MI) during MIS4 and MIS5a. The red line (without P/P) is the reconstructed values once Poaceae and Polypodiales are removed. Removing these two taxa reduces anomalous peaks, where they were particularly abundant, but has little impact on the reconstructions for the rest of the core.

Figure 4: Reconstructed mean temperature of the coldest month (MTCO, °C), growing degree days above a base level of 0° C (GDD_0) and moisture index (the ratio of annual precipitation to annual potential evapotranspiration, MI). Only samples with a Hill's N2 biodiversity index >2 are plotted. The Marine Isotope Stages (MIS) and substages are shown by vertical dotted lines and labelled; we also show the transition interval between MIS6 and MIS5e. Red dots indicate the modern climate calculated from the elevation-corrected climate data from the Climate Research Unit (CRU) CL 2.0 data set.

Figure 5: The correlation of the temperature seasonality and insolation. The black line in the top plot is the normalized difference of reconstructed mean temperature of the coldest month and the mean temperature of the warmest month calculated based on MTCO and GDD_0 (Appendix 1). The orange line in the top plot is the difference between July and January insolation in W m^{-2} at 40.49 °N (the latitude of Villarquemado). The bottom panel shows mid-monthly insolation anomalies (compared to present) in W m^{-2} at 40.49N through time.

Figure 6: Scatter plot showing the impact of the [CO_2] correction on the reconstructed moisture index (MI). The coloured dots represent the implied change in the reconstructions, grouped according to level of the actual [CO_2] at that time (in ppm).

Table 1: Summary statistics for the first three axes of CCA in the whole European data set. The analysis was based on 6458 sites, 196 taxa and three bioclimatic variables: mean temperature of the coldest month (MTCO, °C), growing degree days above 0° C (GDD_0) and the moisture index (MI). We also show the summary statistics for the ANOVA-like permutation test (999 permutations).

Table 2: The results of randomisation *t*-test on the leave-one-out cross-validated predictions of the weighted averaging-partial least squares (WA-PLS) regression

Clim. Past Discuss., https://doi.org/10.5194/cp-2019-16
Manuscript under review for journal Clim. Past
Discussion started: 12 February 2019

models used for the climate reconstructions. The final model is based on 194 taxa, omitting Poaceae and Polypdiales. Selected components in the final model are marked in bold.

Table 3: Reconstructed average values of mean temperature of the coldest month (MTCO, °C), growing degree days above a base level of 0° C (GDD_0) and moisture index (the ratio of annual precipitation to annual potential evapotranspiration, MI) for Marine Isotope Stages (MIS) and substages, calculated from the interpolated yearly values of each variable.

Clim. Past Discuss., https://doi.org/10.5194/cp-2019-16
Manuscript under review for journal Clim. Past
Discussion started: 12 February 2019

Climate of the Past Discussions

Appendix 1

1. An approximation of the dependence of GDD_0 (growing degree days on a zero base) on T_{min} (coldest-month temperature) and T_0 (mean annual temperature)

Assume that temperature (T) follows a sinusoidal pattern with time of year:

$$T = T_0 - \Delta T \cos\theta$$

where ΔT is the half-amplitude of seasonal variation in temperature, and θ is the 'day angle':

$$\theta = (2\pi/365)\, t_d$$

where t_d is the day of the year, measured from a starting point in midwinter. Then:

$$T_{min} = T_0 - \Delta T$$

$$GDD_0 = \int_{T>0} (T_0 - \Delta T \cos\theta)\, d\theta \quad \text{(in units of K rad, where 1 K rad} = 2\pi/365 \text{ K day)}$$

The day-angle when T = 0 is given by $\theta_0 = \cos^{-1}(T_0/\Delta T)$, except in two special cases:

1) $T_0 > \Delta T \Rightarrow GDD_0 = 2\pi T_0$ (this is the case when $T_{min} \geq 0$, hence every day is a growing day)

2) $-T_0 > \Delta T \Rightarrow GDD_0 = 0$ (this is the case when there are no growing days)

Otherwise:

$$GDD_0 = 2 \left[T_0\, \theta - \Delta T \sin\theta \right] \text{ evaluated from } \theta_0 \text{ to } \pi$$

$$= 2\pi T_0 - 2 T_0 \cos^{-1}(T_0/\Delta T) - 2\Delta T [\sin\pi - \sin\cos^{-1}(T_0/\Delta T)]$$

$$= 2\pi T_0 - 2 T_0 \cos^{-1}(T_0/\Delta T) - 2\Delta T \sqrt{[1 - (T_0/\Delta T)^2]}$$

Write $u = T_0/\Delta T$

Then $GDD_0 = 2\Delta T [\pi u - u \cos^{-1} u + \sqrt{(1 - u^2)}]$

$$= 2\Delta T [u \cos^{-1}(-u) + \sqrt{(1 - u^2)}].$$

This is in units of K rad. Multiplication by $365/2\pi$ converts this to units of K day.

2. Predicting T_0 from GDD_0 and T_{min}

From the logic above:

$$-T_{min}/\Delta T = 1 - u \text{ and } GDD_0/\Delta T = 2 [u \cos^{-1}(-u) + \sqrt{(1 - u^2)}]$$

Therefore:

$$-GDD_0/T_{min} = 2 [u \cos^{-1}(-u) + \sqrt{(1 - u^2)}] / (1 - u)$$

Clim. Past Discuss., https://doi.org/10.5194/cp-2019-16
Manuscript under review for journal Clim. Past
Discussion started: 12 February 2019

Climate of the Past Discussions
Open Access
EGU

911 $$= \; 2 \left\{ [(u/(1-u)] \cos^{-1}(-u) + \sqrt{[(1+u)/(1-u)]} \right\}.$$

912 To estimate mean temperature (T_0): convert GDD_0 from K day to K rad, take the ratio
913 of GDD_0 to ($-T_{min}$), and solve the equation above for u. Then,

914 $$T_0 = -T_{min}\, u/(1-u)$$

915 and

916 $$\Delta T = -T_{min}/(1-u).$$

Clim. Past Discuss., https://doi.org/10.5194/cp-2019-16
Manuscript under review for journal Clim. Past
Discussion started: 12 February 2019

Climate of the Past Discussions
Open Access
EGU

Figure 1. Location of modern pollen samples and fossil pollen site. (a) Map of the Iberian Peninsula showing the location of Villarquemado superimposed on a simplified elevation map of the region. (b) Vegetation map of Villarquemado area showing dominant tree species, surface area of the basin and location of the core site. (c) Map showing the location of Villarquemado and the distribution of modern pollen samples. The background map shows mean temperature of the coldest month (MTCO, °C).

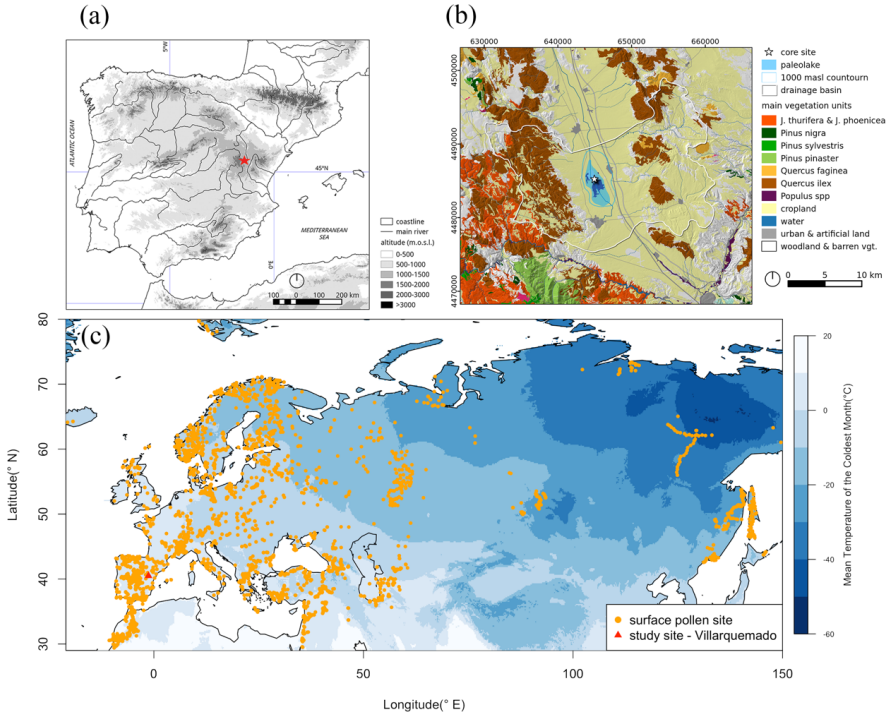

Clim. Past Discuss., https://doi.org/10.5194/cp-2019-16
Manuscript under review for journal Clim. Past
Discussion started: 12 February 2019

Climate of the Past Discussions
Open Access
EGU

Figure 2: Simplified stratigraphic and pollen diagram from Villarquemado. The first column shows changes in stratigraphy, including the alternation between lacustrine and non-lacustrine conditions. The simplified pollen diagram shows the changing abundance of Mediterranean and steppe taxa. We also show the changing abundance of Poaceae and Polypodiales. The final column shows the biodiversity index (Hill's N2).

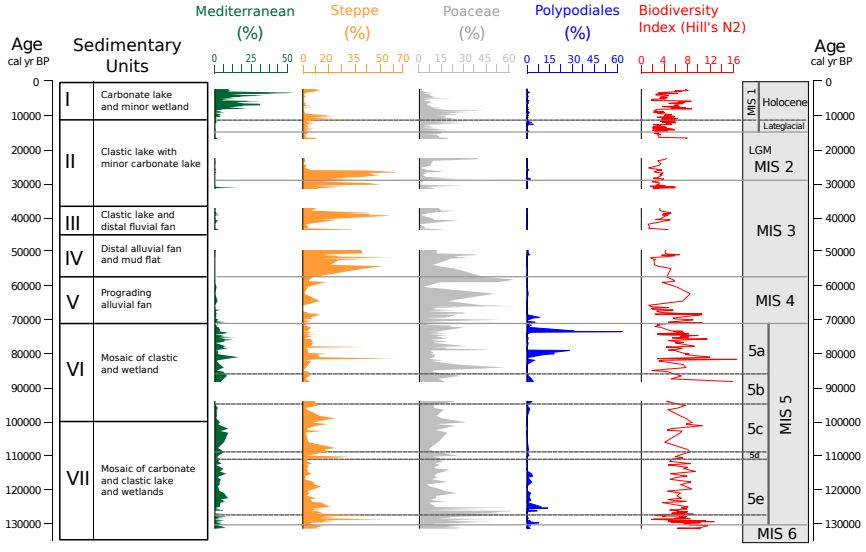

Clim. Past Discuss., https://doi.org/10.5194/cp-2019-16
Manuscript under review for journal Clim. Past
Discussion started: 12 February 2019

Climate of the Past Discussions
Open Access
EGU

934 Figure 3: The impact of removing Poaceae and Polypodiales from the taxon set on
935 reconstructions of moisture index (the ratio of annual precipitation to annual potential
936 evapotranspiration, MI) during MIS4 and MIS5a. The red line (without P/P) is the
937 reconstructed values once Poaceae and Polypodiales are removed. Removing these two
938 taxa reduces anomalous peaks, where they were particularly abundant, but has little
939 impact on the reconstructions for the rest of the core.

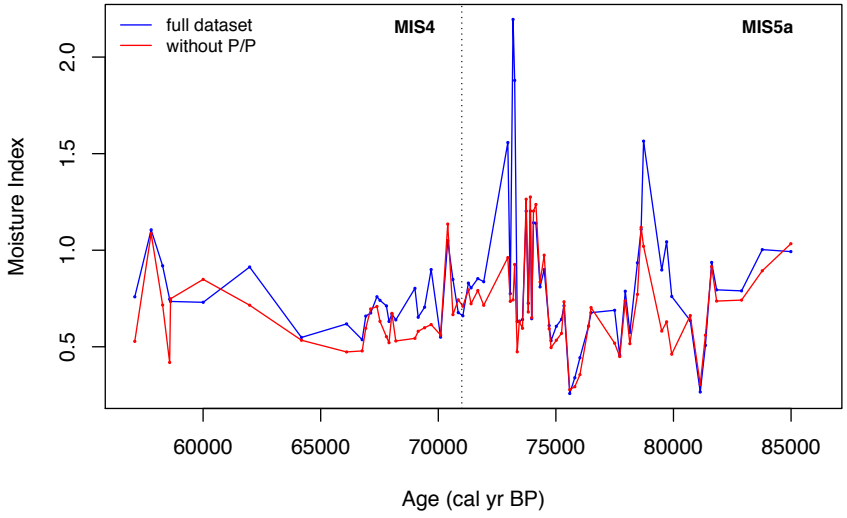

940

Clim. Past Discuss., https://doi.org/10.5194/cp-2019-16
Manuscript under review for journal Clim. Past
Discussion started: 12 February 2019

Climate of the Past Discussions
Open Access
EGU

941 Figure 4: Reconstructed mean temperature of the coldest month (MTCO, °C), growing
942 degree days above a base level of 0° C (GDD_0) and moisture index (the ratio of annual
943 precipitation to annual potential evapotranspiration, MI). Only samples with a Hill's
944 N2 biodiversity index >2 are plotted. The Marine Isotope Stages (MIS) and substages
945 are shown by vertical dotted lines and labelled; we also show the transition interval
946 between MIS6 and MIS5e. Red dots indicate the modern climate calculated from the
947 elevation-corrected climate data from the Climate Research Unit (CRU) CL 2.0 data
948 set.

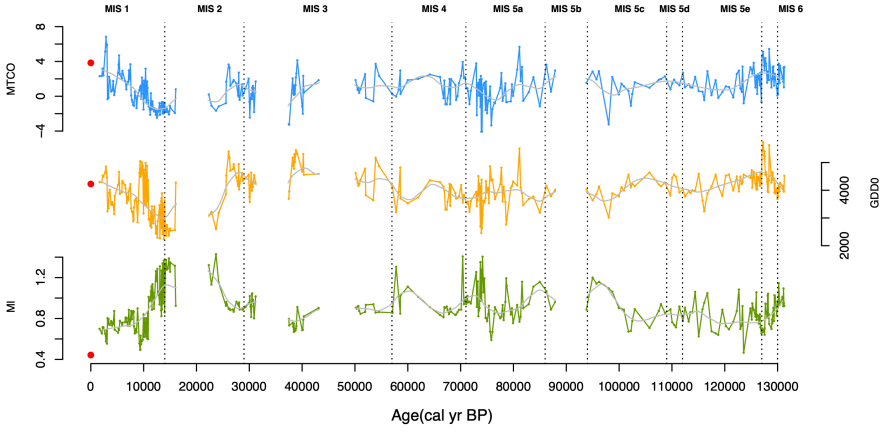

949

Clim. Past Discuss., https://doi.org/10.5194/cp-2019-16
Manuscript under review for journal Clim. Past
Discussion started: 12 February 2019

Climate of the Past Discussions
Open Access
EGU

Figure 5: The correlation of the temperature seasonality and insolation. The black line in the top plot is the normalized difference of reconstructed mean temperature of the coldest month and the mean temperature of the warmest month calculated based on MTCO and GDD_0 (Appendix 1). The orange line in the top plot is the difference between July and January insolation in W m^{-2} at 40.49 °N (the latitude of Villarquemado). The bottom panel shows mid-monthly insolation anomalies (compared to present) in W m^{-2} at 40.49N through time.

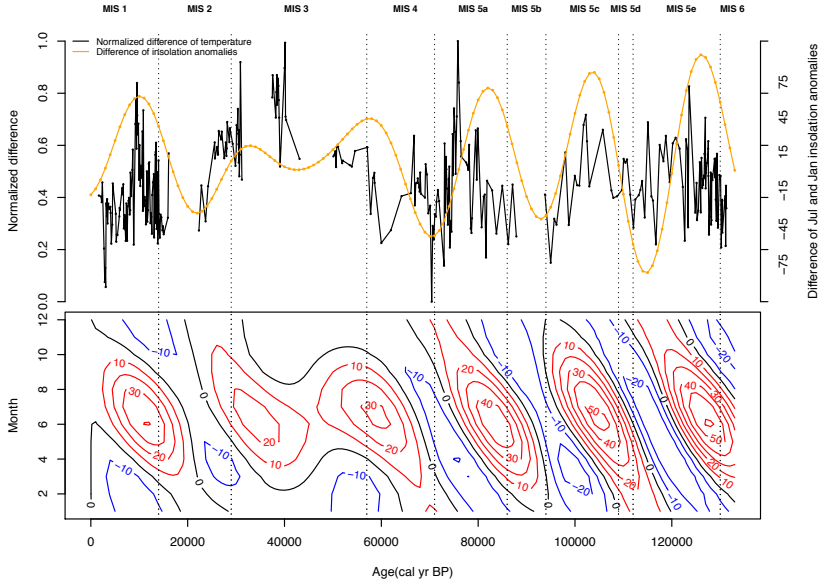

Clim. Past Discuss., https://doi.org/10.5194/cp-2019-16
Manuscript under review for journal Clim. Past
Discussion started: 12 February 2019

Climate of the Past Discussions
Open Access
EGU

958 Figure 6: Scatter plot showing the impact of the [CO_2] correction on the reconstructed
959 moisture index (MI). The coloured dots represent the implied change in the
960 reconstructions, grouped according to level of the actual [CO_2] at that time (in ppm).

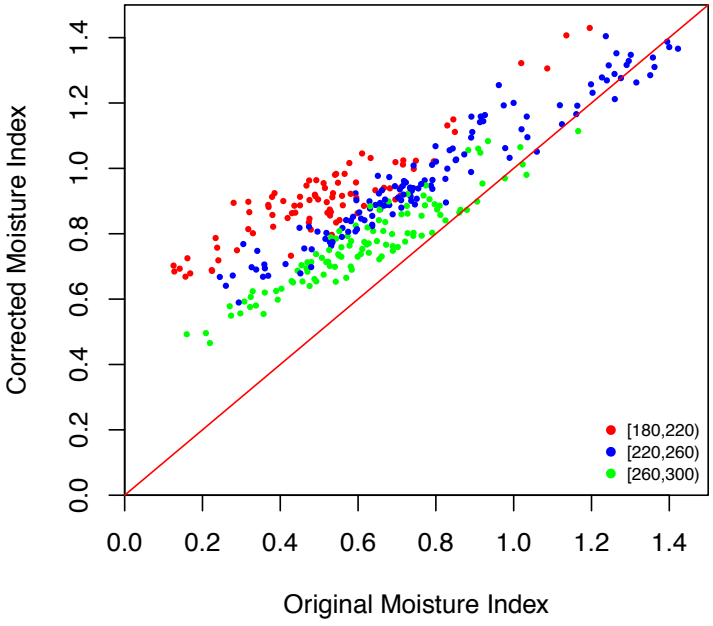

961

Clim. Past Discuss., https://doi.org/10.5194/cp-2019-16
Manuscript under review for journal Clim. Past
Discussion started: 12 February 2019

Climate of the Past Discussions

962 Table 1: Summary statistics for the first three axes of CCA in the whole European data
963 set. The analysis was based on 6458 sites, 196 taxa and three bioclimatic variables:
964 mean temperature of the coldest month (MTCO, °C), growing degree days above 0°C
965 (GDD_0) and the moisture index (MI). We also show the summary statistics for the
966 ANOVA-like permutation test (999 permutations).
967

Axes:	Axis 1	Axis 2	Axis 3	Variance Inflation Factor
Constrained eigenvalues	0.376	0.140	0.060	
Cumulative percentage variance of species-environment relationship	65.4	89.7	100.0	
Species-environment correlations	0.83	0.61	0.47	
Correlations of the environmental variables with the axes:				
MI	0.693	0.594	-0.409	2.28
T_{min}	-0.883	0.456	-0.109	3.21
GDD_0	-0.946	-0.193	-0.260	5.23

	Df	ChiSquare	F	Pr (>F)
Whole model:	3	0.5757	64.393	0.001
Bioclimatic variables:				
MI	1	0.2399	80.506	0.001
MTCO	1	0.2543	85.344	0.001
GDD_0	1	0.0814	27.329	0.001
Aexs:				
CCA 1	1	0.3763	126.253	0.001
CCA 2	1	0.1399	46.956	0.001
CCA 3	1	0.0595	19.971	0.001

968

Clim. Past Discuss., https://doi.org/10.5194/cp-2019-16
Manuscript under review for journal Clim. Past
Discussion started: 12 February 2019

Climate of the Past Discussions

969 Table 2: The results of randomisation *t*-test on the leave-one-out cross-validated
970 predictions of the weighted averaging-partial least squares (WA-PLS) regression
971 models used for the climate reconstructions. The final model is based on 194 taxa,
972 omitting Poaceae and Polypdiales. Selected components in the final model are marked
973 in bold.
974

WA-PLS component	RMSEP	r^2	Maximum bias	p
MTCO				
1	5.308	0.624	13.551	0.001
2	4.967	0.671	9.044	0.001
3	4.852	0.686	8.919	0.001
4	**4.829**	**0.689**	**9.882**	**0.035**
5	4.840	0.688	9.811	0.729
GDD_0				
1	965.106	0.618	2529.455	0.001
2	909.640	0.660	2287.800	0.001
3	892.668	0.673	2195.842	0.001
4	**890.397**	**0.675**	**2278.140**	**0.022**
5	891.459	0.674	2305.115	0.774
MI				
1	0.452	0.444	3.868	0.001
2	0.430	0.497	3.466	0.001
3	**0.427**	**0.505**	**3.439**	**0.004**
4	0.426	0.506	3.497	0.407

975

Clim. Past Discuss., https://doi.org/10.5194/cp-2019-16
Manuscript under review for journal Clim. Past
Discussion started: 12 February 2019

Climate of the Past Discussions
Open Access
EGU

976 Table 3: Reconstructed average values of mean temperature of the coldest month
977 (MTCO, °C), growing degree days above a base level of 0° C (GDD_0) and moisture
978 index (the ratio of annual precipitation to annual potential evapotranspiration, MI) for
979 Marine Isotope Stages (MIS) and substages, calculated from the interpolated yearly
980 values of each variable.
981

	MTCO	GDD_0	MI
MIS1	0.81	3729	0.81
MIS2	-0.22	3631	1.10
MIS3	1.04	4542	0.85
MIS4	1.52	3894	0.97
MIS5a	0.65	3817	0.96
MIS5b	2.08	3955	0.97
MIS5c	1.15	4063	0.92
MIS5d	1.52	4168	0.82
MIS5e	1.25	4182	0.80
MIS6	2.34	4102	0.99

982